



ORIGINAL ARTICLE

Biomolecular interaction and cytotoxicity of ruthenium(III) benzothiazole substituted ferrocenyl thiosemicarbazone complexes



K. Sampath^a, C. Jayabalakrishnan^{b,*}

^a Department of Chemistry, Kumaraguru College of Technology, Coimbatore 641049, Tamil Nadu, India

^b Post-Graduate and Research Department of Chemistry, Sri Ramakrishna Mission Vidyalyaya College of Arts and Science, Coimbatore 641020, Tamil Nadu, India

Received 30 July 2012; accepted 20 December 2013

Available online 29 December 2013

KEYWORDS

Ruthenium(III) complexes;
Benzothiazolyl
thiosemicarbazide;
DNA binding;
DNA cleavage;
Cytotoxicity

Abstract In our search for new anticancer and DNA interacting agents, ruthenium(III) thiosemicarbazone complexes of the type $[\text{RuCl}_2(\text{EPh}_3)\text{L}]$ (where E = P/As; L = monobasic tridentate thiosemicarbazone ligand) were synthesized and characterized by physico-chemical and spectroscopic methods. All the ligands and complexes exhibit noticeable growth inhibition against fungal species and bacterial species. The interactions of these complexes with biomolecule, CT-DNA were investigated by absorbance measurement and gel electrophoresis. Absorption spectral study indicates that the ruthenium(III) complexes have an intrinsic binding constant in the range of $1.0\text{--}3.6 \times 10^4 \text{ M}^{-1}$. The complexes exhibit a remarkable DNA cleavage activity with CT-DNA in the presence of hydroxyl radical. The cleavage activity was carried out with the variation of the concentration of complexes and incubation time. Further, an *in vitro* cytotoxicity study of the complexes exhibited antitumor activity against the HeLa tumor cell line. This research may provide valuable insight into the interactions of metal complexes with DNA and cytotoxicity, knowledge that is an excellent back drop for the rational design of promising drugs.

© 2013 King Saud University. Production and hosting by Elsevier B.V. This is an open access article under the CC BY-NC-ND license (<http://creativecommons.org/licenses/by-nc-nd/3.0/>).

1. Introduction

In the recent years the bioorganometallic chemistry of ferrocene has aroused a great interest and its study has been encouraged by its potential biological applications (Gimeno et al., 2011). The ferrocenyl group has been incorporated into the structure of a number of biologically active molecules such as antibiotic (Edwards et al., 1976), anticancer (Jaouen et al., 2004) or malaria drugs (Biot et al., 2005) resulting in an increase of the activity and these compounds can be used for synthesis of a wide number of pharmacologically active compounds (Azza and Hussien,

* Corresponding author. Tel.: +91 422 2692461.
E-mail address: drcjbstar@gmail.com (C. Jayabalakrishnan).

Peer review under responsibility of King Saud University.



Production and hosting by Elsevier

2009). Ferrocene containing complexes can be regarded as multi nuclear molecules possessing the features of both organometallic and coordination complexes (Jeragh and Dissouky, 2005). Many transition metal complexes of ferrocene derived thiosemicarbazones have been found to be active against pesticides and fungicides (Singh et al., 2002). A complex of thiosemicarbazones has also been screened for medicinal properties, shown to possess some degree of cytotoxic activity (Prabhakaran et al., 2011). It is well known that several metal ions enhance and modify the biological activities of thiosemicarbazones; much attention on the ruthenium atom has been drawn toward the chemistry of ruthenium (Sharma et al., 2007). Ruthenium complexes were used as antitumor agents with selective antimetastatic properties and low systemic toxicity (Trynda-Lemiesz, 2004). Apart from this, ruthenium complexes appear to penetrate reasonably well into the tumor cells and bind effectively to DNA (Chitrapriya et al., 2008) because DNA is generally the primary intracellular target of anticancer drugs. So, the interaction of these drugs with DNA can cause DNA damage in cancer cells and result in cell death (Collinson and Fenton, 1996; Hecht, 2000). In particular, benzothiazolyl thiosemicarbazones represent a very interesting class of compounds because of their wide applications in pharmaceutical aspects such as antibacterial and antifungal (Pandeya et al., 1999). Based on the various activities of these compounds, we have focused on the construction and biological investigation of a novel ruthenium(III) complexes containing benzothiazole substituted ferrocenyl thiosemicarbazones. This paper presents the synthesis, characterization, DNA binding, DNA cleavage and anticancer activity of mixed ligand ruthenium(III) complexes.

2. Experimental

2.1. Materials and methods

All the chemicals used were chemically pure and AR grade. Solvents were purified and dried according to the standard procedure (Vogel, 1989). $\text{RuCl}_3 \cdot 3\text{H}_2\text{O}$ was purchased from Loba Chemie and was used without further purification. Calf-thymus (CT-DNA) was purchased from Bangalore Genei, Bangalore, India. The Human Cervical cancer cell line HeLa was obtained from National centre for cell science (NCCS), Pune, India. The carbon, hydrogen, nitrogen and sulfur analyses were performed on a Vario EL III CHNS analyser at STIC, Cochin University of Science and Technology, Kerala, India. IR spectra were recorded as KBr pellets in the $400\text{--}4000\text{ cm}^{-1}$ region using Perkin Elmer FTIR 8000 spectrophotometer. Electronic spectra were recorded in dimethyl sulphoxide solution with a Systronics double beam UV-vis spectrophotometer 2202 in the range $200\text{--}800\text{ nm}$. Magnetic susceptibility measurements of the complexes were recorded using Guoy balance. EPR spectra were recorded on a varian E-112 ESR spectrophotometer at X-band microwave frequencies for powdered samples at room temperature and liquid nitrogen temperature at the Indian Institute of Technology, Bombay, Mumbai. Anti cancer studies were carried out at the Kovai Medical Centre and Hospital Pharmacy College, Coimbatore, Tamil Nadu. Melting points were recorded on a Veego VMP-DS model heating table and were not corrected. The thiosemicarbazone ligands (Sampath and Jayabalakrishnan, 2013) and the metal precursors $[\text{RuCl}_3(\text{PPh}_3)_3]$ (Chatt et al., 1968) and $[\text{RuCl}_3(\text{AsPh}_3)_3]$

(Thangadurai and Natarajan, 2001) were prepared according to the reported procedures.

2.2. Synthesis of thiosemicarbazone ligands

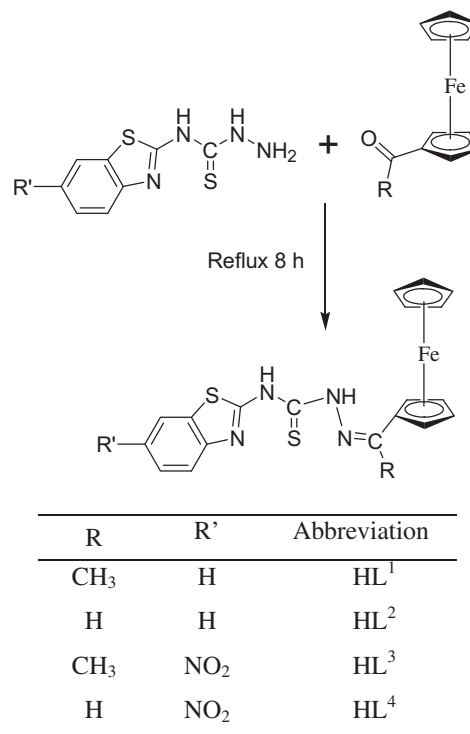
A solution of 6-nitro/H-2-benzothiazolyl thiosemicarbazide (2.24–2.69 g, 10 mmol) in methanol (20 mL) was added to a solution of ferrocene carboxaldehyde/acetyl ferrocene (2.14–2.28 g, 10 mmol) in methanol (20 mL) along with a few drops of glacial acetic acid. The mixture was refluxed for 8 h. The resultant product was washed with methanol and the purity of the ligands was checked by TLC. The outline synthesis of thiosemicarbazone ligands is shown in Scheme 1.

2.3. Synthesis of ruthenium(III) thiosemicarbazone complexes

All the reactions were carried out under strictly anhydrous condition. The monobasic tridentate thiosemicarbazones (0.042–0.048 g, 0.1 mmol) were added to a solution of $[\text{RuCl}_3(\text{EPh}_3)_3]$, (E = P/As) (0.090–0.113 g) in 1:1 M ratio in benzene-methanol/tetrahydrofuran (50 mL) mixture, and then refluxed for 7 h. The resulting solution was concentrated to about 3 cm^3 and the complexes were precipitated by the addition of a small quantity of petroleum ether ($60\text{--}80\text{ }^\circ\text{C}$). The complexes were then filtered off, washed with petroleum ether and recrystallized from tetrahydrofuran/ CH_2Cl_2 /petroleum ether and dried under *vacuo*.

2.4. Antimicrobial assay

The agar diffusion method was followed for antibacterial and antifungal susceptibility tests. Petri plates were prepared by pouring 10 mL of Mueller Hinton Agar for bacteria and allowed to solidify. These agar plates were inoculated with



Scheme 1 Outline synthesis of the thiosemicarbazone ligands.

0.1 mL of a standardized bacterial suspension (2×10^6 cells mL⁻¹) and uniformly spread. A 6 mm well was cut at the center of the agar plate and the well was filled with the solution of the complexes. The diameter of the inhibition zone observed around the well was measured for each bacterium after 24 h of incubation at 37 °C. One well was filled with sterile distilled water to serve as a control. For fungus, Sabouraud Dextrose Agar medium was amended with the complexes when the medium was warm, and poured into petri plates. After solidification of the medium, mycelia disks (6 mm diameter) of the test fungi were inoculated at the center of the plates. The diameter of the inhibition zone for each fungus was measured after 48 h of incubation at 28 °C.

2.5. DNA-binding and cleavage assay

2.5.1. Electronic absorption spectroscopy

All the experiments involving the binding of ruthenium(III) complexes with CT-DNA were carried out in a double distilled water buffer with tris(hydroxymethyl)-aminomethane (Tris, 5 mM) and sodium chloride (50 mM) and adjusted to pH 7.2 with hydrochloric acid. A solution of CT-DNA in the buffer gave a ratio of UV absorbance of about 1.9 at 260 and 280 nm, indicating that the DNA was sufficiently free of protein. The compounds were dissolved in a mixed solvent of 5% DMSO and 95% Tris-HCl buffer. Absorption titration experiments were performed with fixed concentrations of the compounds (20 μM) with varying concentration of DNA (0–40 μM). While measuring the absorption spectra, an equal amount of DNA was added to both the test solution and the reference solution to eliminate the absorbance of DNA itself. The values of the intrinsic binding constants K_b were calculated by regression analysis using the equation (Wolfe et al., 1987).

$$[\text{DNA}]/(\epsilon_a - \epsilon_f) = [\text{DNA}]/(\epsilon_b - \epsilon_f) + 1/K_b(\epsilon_a - \epsilon_f)$$

where [DNA] is the concentration of CT-DNA in base pairs and ϵ_a , ϵ_f and ϵ_b are extinction coefficients of the apparent, free and bound metal complex, respectively and K_b is the equilibrium binding constant in M⁻¹. In the plots of $[\text{DNA}]/(\epsilon_a - \epsilon_f)$ versus [DNA], K_b is given by the ratio of slope to the intercept.

2.5.2. DNA cleavage

The DNA cleavage activity of the ruthenium(III) complexes was monitored by agarose gel electrophoresis on CT DNA. The tests were performed under aerobic condition with H₂O₂ as an oxidant. Each reaction mixture contained 30 μM of CT DNA, 30 and 60 μM of each complex in DMSO and 60 μM of hydrogen peroxide in 50 mM Tris-HCl, (pH 7.1). The reaction mixture was incubated for 2 h and 4 h at 37 °C. After incubation, 1 μL of loading buffer (0.25% bromophenol blue, 0.25% xylene cynol and 60% glycerol) was added to the reaction mixture and loaded onto a 1% agarose gel containing 1.0 μg/mL of ethidium bromide. The electrophoresis was carried out in Tris-acetic acid EDTA buffer at 50 V. The bands were visualized under UV light and photographed.

2.6. Cytotoxicity assay

The human cervical cancer cell line (HeLa) was obtained from the National Centre for Cell Science (NCCS), Pune, and grown

in Eagles Minimum Essential Medium containing 10% fetal bovine serum (FBS). All cells were maintained at 37 °C, 5% CO₂, 95% air and 100% relative humidity. Maintenance cultures were passaged weekly, and the culture medium was changed twice a week.

The monolayer cells were detached with trypsin-ethylene-diaminetetraacetic acid (EDTA) to make single cell suspensions and viable cells were counted using a hemocytometer and diluted with medium with 5% FBS to give a final density of 1×10^5 cells/mL. One hundred microliters per well of cell suspension were seeded into 96-well plates at a plating density of 10,000 cells/well and incubated to allow for cell attachment at 37 °C, 5% CO₂, 95% air and 100% relative humidity. After 24 h the cells were treated with serial concentrations of the extracts and fractions. They were initially dissolved in neat DMSO and further diluted in serum free medium to produce various concentrations. One hundred microliters per well of each concentration was added to plates to obtain final concentrations of 1.0, 0.5, 0.25, 0.125, and 0.063 μg/mL. The final volume in each well was 200 μL and the plates were incubated at 37 °C, 5% CO₂, 95% air and 100% relative humidity for 48 h. The medium containing without samples were used as control. Triplicate runs were carried out for all concentrations.

3-(4,5-Dimethylthiazol-2-yl)-2,5-diphenyl tetrazolium bromide (MTT) is a yellow water soluble tetrazolium salt. A mitochondrial enzyme in living cells, succinate-dehydrogenase, cleaves the tetrazolium ring, converting the MTT to an insoluble purple formazan. Therefore, the amount of formazan produced is directly proportional to the number of viable cells. After 48 h of incubation, 15 μL of MTT (5 mg/mL) in phosphate buffered saline (PBS) was added to each well and incubated at 37 °C for 4 h. The medium with MTT was then flicked off and the formed formazan crystals were solubilized in 100 μL of DMSO and then the absorbance at 570 nm was measured using a micro plate reader. The % cell inhibition was determined using the following formula.

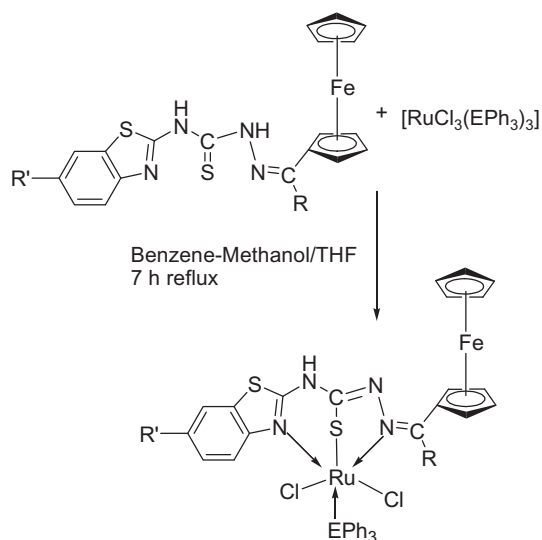
$$\% \text{Growth Inhibition} = 100 - \text{Abs}(\text{sample})/\text{Abs}(\text{control}) \times 100.$$

Nonlinear regression graph was plotted between % Cell inhibition and Log₁₀ concentration and IC₅₀ was determined using GraphPad Prism software (Monks et al., 1991).

3. Results and discussion

A new series of ruthenium(III) thiosemicarbazone complexes of the type [RuCl₂(EPh₃)L] (E = P/As; L = monobasic tridentate thiosemicarbazone ligands) were achieved by reacting ruthenium(III) precursors [RuCl₃(EPh₃)₃] with monobasic tridentate thiosemicarbazone ligands in 1:1 M ratio, respectively in benzene-methanol/tetrahydrofuran mixture (Scheme 2).

The synthesized ruthenium(III) thiosemicarbazone complexes are stable in air at room temperature, non-hygroscopic in nature and soluble in common solvents such as dichloromethane, dimethyl formamide, dimethyl sulphoxide, etc. The analytical data of the complexes are in good agreement with the calculated values thus confirming the proposed hetero bimetallic composition for all the complexes (Table 1).



Where E=P/As; R=H/CH₃; R'=H/NO₂

Scheme 2 Formation of ruthenium(III) thiosemicarbazone complexes.

3.1. IR spectroscopy

The important IR absorption frequencies of the synthesized complexes are shown in Table 2. The free ligands display $\nu_{(C=S)}$ absorptions in the region 804–826 cm^{-1} , shifts to 723–746 cm^{-1} in the spectra of the complexes. This observation may be attributed to the enolization of $-\text{NH}-\text{C}=\text{S}$ and subsequent coordination through deprotonated sulfur (Mahalingam et al., 2010). The ligands showed a strong band in the range 1632–1642 cm^{-1} which is characteristic of the azomethine group $\nu_{(C=N)}$. Coordination of the thiosemicarbazone to the ruthenium atom through the azomethine nitrogen atom is expected to reduce the electron density in the azomethine link and thus lowers the $\nu_{(C=N)}$ absorption frequency in the region 1610–1639 cm^{-1} (Bechford et al., 2009). IR spectrum of the ligands revealed a medium intensity band in the region 1514–1593 cm^{-1} $\nu_{(C=N)}$ of the thiazole ring, which is shifted to lower frequency in the range 1457–1557 cm^{-1} after complexation, which also indicates that it has been affected upon coordination to the metal ions (Prasad et al., 2010). The $\nu_{(C-S-C)}$ at 616–618 cm^{-1} of the thiazole ring remains unchanged which demonstrated that the thiazole group of sulfur does not coordinate to the ruthenium metal (Alam et al.,

2008). Absorptions at 474–545 cm^{-1} and 423–458 cm^{-1} in the spectra of the complexes are attributed to the $\nu_{(Ru-N)}$ and $\nu_{(Ru-S)}$ vibrations (Manivannan et al., 2007). The band at 486–491 cm^{-1} was assigned to the $\nu_{(Fe-Cp)}$ stretching frequency (Abd-Elzاهر and Ali, 2006). In addition, other characteristic bands due to triphenylphosphine/triphenylarsine are also present in the expected region.

3.2. Electronic spectra

The electronic absorption spectra of the free ligands and their complexes were recorded in DMSO and the UV-vis data were listed in Table 2. The ground state of ruthenium(III) is $^2T_{2g}$ and first existed doublet levels in the order of increasing energy are $^2A_{2g}$ and $^2A_{1g}$, which arise from $t_{2g}^4 e_g^1$ configuration (Venkatachalam et al., 2008). The spectra of the free ligands showed the two type of transitions appearing in the range 298–305 and 368 nm are due to $\pi-\pi^*$ and $n-\pi^*$ transitions involving molecular orbital of the cyclopentadienyl ring, C=N and enolic $-\text{SH}$ chromophore. The shoulder in the region 430–447 nm is attributed to the transition of 3d electron on iron to either non-bonding or antibonding orbitals of the cyclopentadienyl ring (Prabhakaran et al., 2011). These bands were shifted in the spectra of the complexes. The ruthenium(III) complexes in the visible region display a strong band in the range 394–416 nm that is assigned to be the LMCT transitions (Muthukumar et al., 2010a,b). In a d^5 system, especially in ruthenium(III) which has relatively high oxidizing properties, the charge transfer bands of the type $L_{\pi y} \rightarrow T_{2g}$ are prominent in the low energy region, which obscures the weaker bands due to d-d transitions. The absorption between 440–480 nm is attributed to MLCT from Fe to either the non-bonding or antibonding orbitals of the cyclopentadienyl ring (Prabhakaran et al., 2011). The lower wavelength bands are characterized as ligand centered transitions occurring within the ligand orbitals. The patterns of the electronic spectra of all the complexes indicate the presence of an octahedral environment around the ruthenium atom (Muthukumar et al., 2010a,b).

3.3. Magnetic moment

The magnetic moment for all the complexes has been measured at room temperature using the Guoy balance. The values obtained in the range 1.62–1.69 BM indicates the presence of one unpaired electron, suggesting a low spin t_{2g}^5 configuration for all the ruthenium(III) atoms in octahedral environment (Muthukumar et al., 2010a,b).

Table 1 Analytical data of ruthenium(III) thiosemicarbazone complexes.

Complexes	Color	Mol. mass	Decomposition temperature (°C)	Calculated (found) (%)			
				C	H	N	S
[RuCl ₂ (PPh ₃)L ¹]	Black	867	> 300	52.60(52.32)	3.72(3.57)	6.46(6.23)	7.39(7.42)
[RuCl ₂ (AsPh ₃)L ¹]	Brown	911	> 300	50.07(50.27)	3.54(3.72)	6.15(6.10)	7.03(7.78)
[RuCl ₂ (PPh ₃)L ²]	Brown	853	> 300	52.06(52.47)	3.54(3.49)	6.56(6.46)	7.51(7.21)
[RuCl ₂ (AsPh ₃)L ²]	Black	897	> 300	49.51(49.18)	3.37(3.76)	6.24(6.83)	7.15(7.46)
[RuCl ₂ (PPh ₃)L ³]	Black	912	> 300	50.01(50.62)	3.42(3.73)	7.67(7.23)	7.03(7.64)
[RuCl ₂ (AsPh ₃)L ³]	Black	956	> 300	47.71(47.18)	3.27(3.75)	7.32(7.69)	6.70(6.13)
[RuCl ₂ (PPh ₃)L ⁴]	Brown	898	> 300	49.46(49.28)	3.25(3.31)	7.79(7.42)	7.14(7.64)
[RuCl ₂ (AsPh ₃)L ⁴]	Brown	942	> 300	47.15(47.53)	3.10(3.78)	7.43(7.53)	6.80(6.19)

Table 2 IR and electronic data of ligands and ruthenium(III) thiosemicarbazone complexes.

Ligands and complexes	FTIR (cm ⁻¹)							UV-vis (nm)	
	ν(C=N)	ν(C=S)	ν(C-S)	Thiazole		ν(Ru-N)	ν(Ru-S)		ν(Fe-Cp)
				ν(C=N)	ν(C-S)				
^a H L ¹	1642	804	–	1524	618	–	–	487	298, 368, 447
^a H L ²	1633	820	–	1593	618	–	–	488	305, 368, 447
^a H L ³	1632	821	–	1516	617	–	–	489	300, 368, 430
^a H L ⁴	1635	826	–	1514	616	–	–	486	305, 368, 437
[RuCl ₂ (PPh ₃)L ¹]	1635	–	723	1457	618	545	458	490	310, 368, 406, 476
[RuCl ₂ (AsPh ₃)L ¹]	1639	–	741	1472	617	474	457	489	308, 368, 411, 440
[RuCl ₂ (PPh ₃)L ²]	1628	–	723	1557	617	540	457	487	305, 368, 394, 444
[RuCl ₂ (AsPh ₃)L ²]	1616	–	742	1545	618	538	458	486	305, 368, 396, 476
[RuCl ₂ (PPh ₃)L ³]	1628	–	745	1472	617	527	424	488	305, 368, 413, 480
[RuCl ₂ (AsPh ₃)L ³]	1626	–	744	1478	617	537	457	491	308, 368, 413, 478
[RuCl ₂ (PPh ₃)L ⁴]	1610	–	746	1461	617	540	426	490	308, 368, 416, 478
[RuCl ₂ (AsPh ₃)L ⁴]	1612	–	744	1483	616	522	423	490	308, 368, 413, 480

^a Reported value.

3.4. EPR spectra

The room temperature and liquid nitrogen temperature EPR spectra of powder samples were recorded at X-band frequencies and the spectral data are given in Table 3. The EPR spectrum of the complex [RuCl₂(AsPh₃)L¹] recorded at room temperature is shown in Fig. 1. [RuCl₂(AsPh₃)L¹] exhibits three lines with different 'g' values $g_x = 2.53$, $g_y = 2.57$ and $g_z = 2.21$ indicating the presence of magnetic anisotropy. The presence of three 'g' values is indicative of a rhombic distortion in this complex. Moreover the complexes, [RuCl₂(AsPh₃)L²] and [RuCl₂(PPh₃)L³] exhibit a characteristic of an axially symmetric system with g_{\perp} around 2.42 and 2.82 and g_{\parallel} around 1.89 and 2.31. For an octahedral field with tetragonal distortion $g_x = g_y \neq g_z$ and hence two 'g' values indicate tetragonal distortion in these complexes (Venkatachalam and Ramesh, 2005). All other ruthenium(III) complexes exhibit a single isotropic resonance with 'g' values in the range 2.55–2.67, indicating very high symmetry around the ruthenium atom; such isotropic lines are usually observed either due to intermolecular spin exchange which can broaden the lines or occupancy of the unpaired electrons in a degenerate orbital (Raja and Ramesh, 2010). EPR spectra recorded for complexes

[RuCl₂(AsPh₃)L¹] and [RuCl₂(PPh₃)L³] at liquid nitrogen temperature did not show much variation from the observed at room temperature, indicating anisotropic resonance in this complex. Furthermore, the position and nature of the lines in the spectra of these complexes are similar to those of the other octahedral ruthenium(III) complexes (Manimaran et al., 2011; Raja and Ramesh, 2010).

3.5. Antimicrobial activity

The antimicrobial activities of the free ligands and the thiosemicarbazone complexes were tested against the pathogenic fungus (*Aspergillus ochraceous*, *Paecilomyces variotii* and *Botrytis Cineriaia*) and human pathogens (*Escherichia coli*, *Staphylococcus aureus* and *Klebsiella pneumonia*). The screening data are reported in Table 4. Ruthenium chelates possess higher antimicrobial activity than the respective free ligands. The inhibition of fungal cells by ruthenium chelates is due to the alteration in the cell permeability and subsequent injury to the cell membrane (Raja et al., 2011; Leelavathy et al., 2009). The inhibition activity of ruthenium chelates against the bacteria suggesting that chelation facilitates the ability of a complex to cross a cell membrane (Perez et al., 1990). Furthermore, the mode of action of the compounds may involve the hydrogen bond through >C=N group with active centers of all cell constituents resulting in interference with the normal cell process (Arunachalam et al., 2010). The present system possess better cytotoxicity than the other ruthenium complexes (Manimaran et al., 2011). Even though the complexes possess higher activity than the free ligands, they could not reach the effectiveness of the standard drugs *Cotrimazole* and *Ciprofloxacin*.

3.6. DNA-binding and cleavage assay

3.6.1. Electronic absorption spectroscopy

DNA-binding studies are important for the rational design and construction of new and more efficient drugs targeted to DNA. Electronic absorption spectroscopy is one of the most useful techniques for DNA-binding studies of metal

Table 3 EPR spectral data of ruthenium(III) thiosemicarbazone complexes.

Complexes	g_x	g_y	g_z	$\langle g \rangle^*$
[RuCl ₂ (PPh ₃)L ¹]	2.57	2.57	2.57	2.57
[RuCl ₂ (AsPh ₃)L ¹]	2.53	2.57	2.21	2.43
[RuCl ₂ (AsPh ₃)L ¹] LNT	2.52	2.56	2.21	2.43
[RuCl ₂ (PPh ₃)L ²]	2.67	2.67	2.67	2.67
[RuCl ₂ (AsPh ₃)L ²]	2.42	2.42	1.89	2.24
[RuCl ₂ (PPh ₃)L ³]	2.82	2.82	2.31	2.65
[RuCl ₂ (PPh ₃)L ³] LNT	2.71	2.71	2.33	2.58
[RuCl ₂ (AsPh ₃)L ³]	2.56	2.56	2.56	2.56
[RuCl ₂ (PPh ₃)L ⁴]	2.62	2.62	2.62	2.62
[RuCl ₂ (AsPh ₃)L ⁴]	2.55	2.55	2.55	2.55

LNT – spectra recorded at liquid nitrogen temperature.

* $\langle g \rangle = [1/3g_x^2 + 1/3g_y^2 + 1/3g_z^2]^{1/2}$.

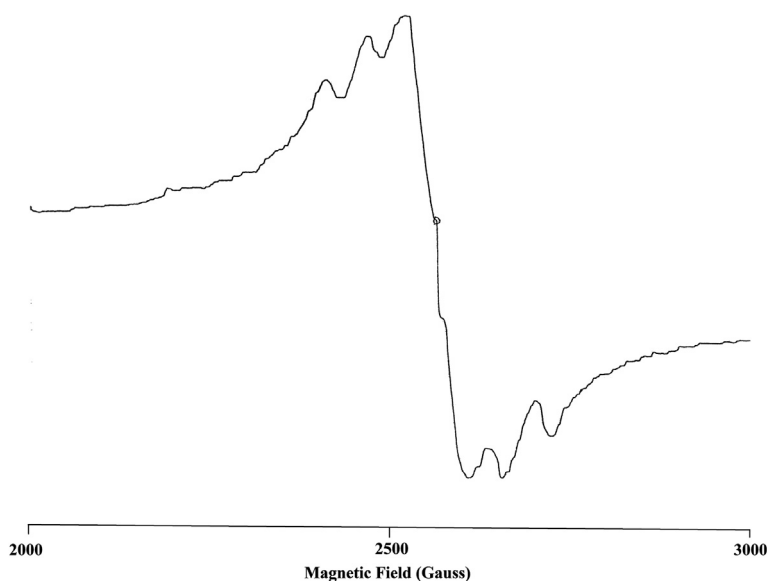


Figure 1 EPR spectrum of $[\text{RuCl}_2(\text{AsPh}_3)\text{L}^1]$.

Table 4 Antimicrobial activity of ruthenium(III) thiosemicarbazone complexes.

Ligands and complexes	Mean zone of inhibition (mm) ^a					
	Bacteria			Fungi		
	<i>E. coli</i>	<i>Staphylococcus aureus</i>	<i>Klebsiella pneumoniae</i>	<i>Aspergillus ochraceous</i>	<i>Pacilomyces variotii</i>	<i>Botrytis cineraia</i>
H L ¹	14.7	15.2	15.1	14.5	13.3	15.6
H L ²	11.4	10.4	13.1	13.6	12.7	13.3
H L ³	13.7	14.8	11.9	15.9	13.6	15.8
H L ⁴	10.6	10.6	12.6	11.9	12.3	12.6
$[\text{RuCl}_2(\text{PPh}_3)\text{L}^1]$	19.6	19.8	19.4	20.1	19.9	19.2
$[\text{RuCl}_2(\text{AsPh}_3)\text{L}^1]$	18.6	18.6	18.3	19.6	19.1	18.5
$[\text{RuCl}_2(\text{PPh}_3)\text{L}^2]$	17.4	17.1	17.8	19.1	16.9	–
$[\text{RuCl}_2(\text{AsPh}_3)\text{L}^2]$	16.5	16.5	16.5	18.5	–	16.2
$[\text{RuCl}_2(\text{PPh}_3)\text{L}^3]$	18.9	17.4	18.2	19.3	18.2	17.9
$[\text{RuCl}_2(\text{AsPh}_3)\text{L}^3]$	17.6	–	17.5	–	17.4	17.1
$[\text{RuCl}_2(\text{PPh}_3)\text{L}^4]$	17.1	16.9	17.2	17.2	16.5	16.4
$[\text{RuCl}_2(\text{AsPh}_3)\text{L}^4]$	16.5	15.8	16.4	16.7	15.7	15.9
Standards ^b	26	24	23	33	32	34
DMSO	No activity					

^a Values are the mean diameter of inhibition zone (mm) and an average of triplicate runs.

^b Standards: antibacterial studies – ciprofloxacin 5 µg/mL; antifungal studies – cotrimazole – 100 µg/mL. Ligands and Complexes concentration were 150 µg/mL.

complexes. The spectral changes reflect the corresponding changes in DNA in its conformation and structures after the drug bound to DNA (Wang and Yang, 2005). Intercalative mode of binding usually results in hypochromism and bathochromism due to strong stacking interaction between an aromatic chromophore and the base pairs of DNA. On the other hand, metal complexes which non-intercalatively or electrostatically bind with DNA may result in hyperchromism and hypsochromism (Lawrence et al., 2006). The electronic spectrum of complexes, $[\text{RuCl}_2(\text{PPh}_3)\text{L}^1]$, $[\text{RuCl}_2(\text{AsPh}_3)\text{L}^2]$, $[\text{RuCl}_2(\text{PPh}_3)\text{L}^3]$ and $[\text{RuCl}_2(\text{PPh}_3)\text{L}^4]$ in the presence and absence of DNA is shown in Fig. 2. The ruthenium(III) complexes exhibit two bands in the region around 252–363 nm, which is attributed to a $\pi-\pi^*$ intraligand transition. The

absorption spectra show clearly that the addition of DNA to the complexes lead to strong hyperchromism accompanied by the slight hypsochromism to the $[\text{DNA}]/[\text{Ru}]$. Obviously, these spectral characteristics suggest that all the complexes interact with DNA via electrostatically with the base pairs of DNA. In order to evaluate quantitatively the DNA-binding strength, the intrinsic DNA-binding constant, K_b , of the ruthenium(III) complexes has been estimated to be in the range $1.0 \times 10^4 \text{ M}^{-1}$ – $3.6 \times 10^4 \text{ M}^{-1}$ and is listed in the Table 5. This is good agreement with the reported literatures (Liu et al., 2005).

As the concentration of the DNA was increased, the absorption intensity of $[\text{RuCl}_2(\text{AsPh}_3)\text{L}^2]$ decreases initially and on further increment, hyperchromism with slight blue shift

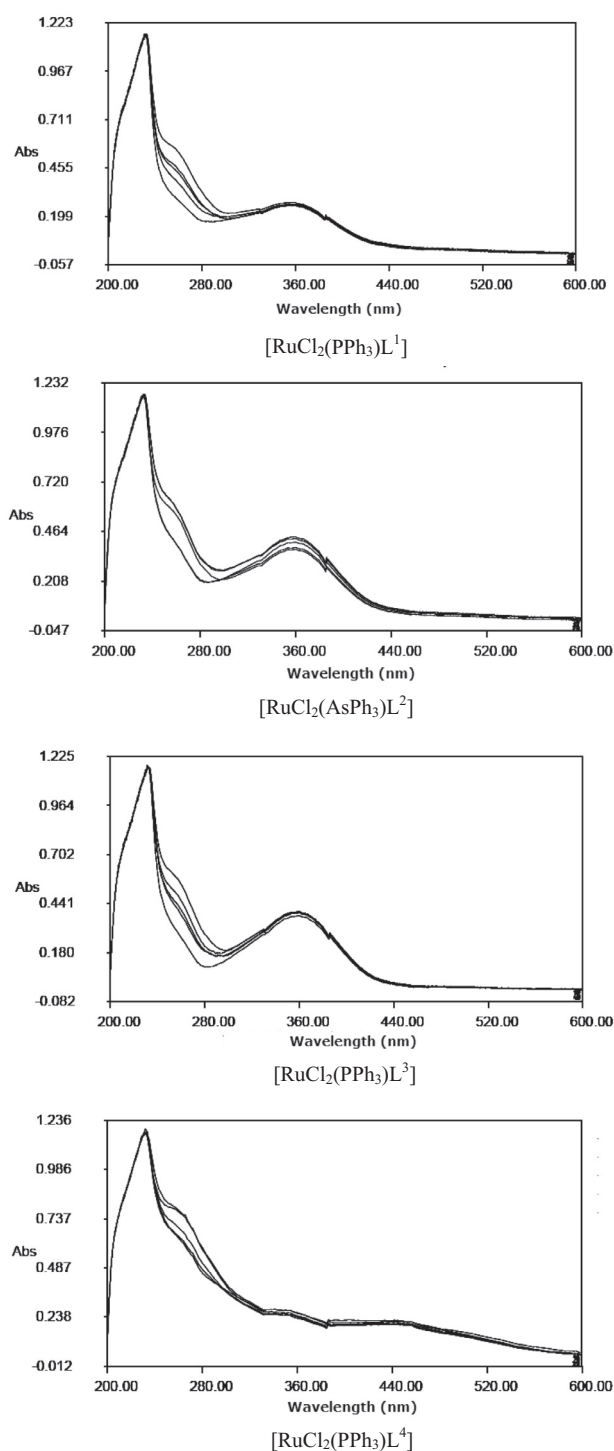


Figure 2 Absorption spectral traces of the complexes $[\text{RuCl}_2(\text{PPh}_3)\text{L}^1]$, $[\text{RuCl}_2(\text{AsPh}_3)\text{L}^2]$, $[\text{RuCl}_2(\text{PPh}_3)\text{L}^3]$ and $[\text{RuCl}_2(\text{PPh}_3)\text{L}^4]$ with increasing concentration of CT-DNA in a Tris HCl–NaCl buffer (pH 7.2).

(5 nm) was observed. This behavior reveals an electrostatic association of the complex with the helix surface (Chitrapriya et al., 2010). Hyperchromicity and hypochromicity is the spectral feature of DNA concerning its double helix structure. Hyperchromic effect reflects the corresponding changes of DNA in its conformation and structure after the complexes

Table 5 Absorption spectral properties of ruthenium(III) complexes with DNA.

Complexes	$K_b \times 10^4 \text{ M}^{-1}$
$[\text{RuCl}_2(\text{PPh}_3)\text{L}^1]$	1.0
$[\text{RuCl}_2(\text{AsPh}_3)\text{L}^1]$	1.6
$[\text{RuCl}_2(\text{PPh}_3)\text{L}^2]$	1.5
$[\text{RuCl}_2(\text{AsPh}_3)\text{L}^2]$	a
$[\text{RuCl}_2(\text{PPh}_3)\text{L}^3]$	1.5
$[\text{RuCl}_2(\text{AsPh}_3)\text{L}^3]$	1.0
$[\text{RuCl}_2(\text{PPh}_3)\text{L}^4]$	3.6
$[\text{RuCl}_2(\text{AsPh}_3)\text{L}^4]$	1.4

^aCould not be evaluated.

are bound to DNA. Hypochromism results from contraction of DNA in the helix axis while hyperchromism results from the damage of DNA helix structure. The binding constant of the complex, $[\text{RuCl}_2(\text{AsPh}_3)\text{L}^2]$ could not be evaluated due to the random changes in the absorption on the addition of DNA.

3.6.2. DNA cleavage activity

The metal complexes were able to cleave the DNA and the efficiency of the complexes compared with that of the control is due to their efficient DNA binding ability. The general oxidative mechanisms proposed to account for DNA cleavage by hydroxyl radicals *via* abstraction of a hydrogen atom from sugar units and prediction of the release of specific residues arising from transformed sugars, depend on the position from which the hydrogen atom is removed (Pratival et al., 1991).

In the present study, the CT-DNA gel electrophoresis experiment was carried out for the complexes, $[\text{RuCl}_2(\text{AsPh}_3)\text{L}^1]$, $[\text{RuCl}_2(\text{PPh}_3)\text{L}^2]$, $[\text{RuCl}_2(\text{PPh}_3)\text{L}^3]$ and $[\text{RuCl}_2(\text{PPh}_3)\text{L}^4]$. The complexes were selected for DNA cleavage activity because these complexes exhibited higher binding affinity in our DNA binding study. The DNA cleaving ability of the complexes has been investigated with various concentrations of the complexes and at 2 h incubation time intervals in the presence of H_2O_2 as an oxidant. Control experiment using DNA alone and DNA with H_2O_2 (Lane 1 and 2) does not show any significant cleavage of CT-DNA even on longer exposure time. From the Fig. 3, it was found that, at very low concentration, few complexes exhibit nuclease activity in the presence of H_2O_2 . When the concentration increased to 60 μM for all the complexes, DNA was completely damaged (Lane 3–10). This proves the catalytic role of complexes in the oxidative cleavage (Reddy et al., 2011).

As can be seen from the Fig. 4, the amount of cleavage is found to increase with increasing incubation time to 4 h, even though the concentration of the complexes is 30 μM (Lane 3–10). The amount of Form I diminished gradually, partly converted to Form II and the intensity of the DNA decreased, showing the potential chemical nuclease activity of the complexes. Hence, we conclude that the ruthenium(III) complexes cleaves DNA at different concentrations and at various incubation time intervals in the presence of H_2O_2 .

3.7. Cytotoxic activity evaluation

To test the cytotoxicity of ruthenium(III) complexes, $[\text{RuCl}_2(\text{AsPh}_3)\text{L}^1]$, $[\text{RuCl}_2(\text{PPh}_3)\text{L}^2]$, $[\text{RuCl}_2(\text{PPh}_3)\text{L}^3]$ and $[\text{RuCl}_2(\text{PPh}_3)\text{L}^4]$ human cervical cancer cell line (HeLa) was cultured

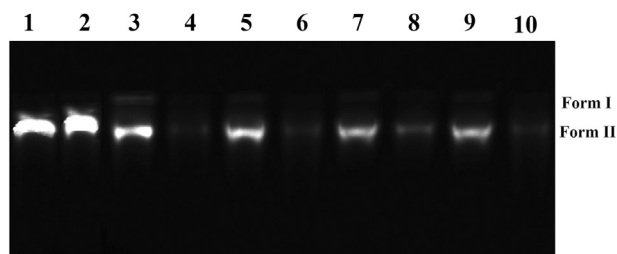


Figure 3 The gel electrophoresis showing the chemical nuclease activity of CT-DNA incubated at 37 °C for 2 h with different concentration of complexes in the presence of H₂O₂ as an oxidant; Lane 1: DNA alone; Lane 2: DNA + 60 μM H₂O₂; Lane 3: DNA + 60 μM H₂O₂ + 30 μM [RuCl₂(AsPh₃)L¹]; Lane 4: DNA + 60 μM H₂O₂ + 60 μM [RuCl₂(AsPh₃)L¹]; Lane 5: DNA + 60 μM H₂O₂ + 30 μM [RuCl₂(PPh₃)L²]; Lane 6: DNA + 60 μM H₂O₂ + 60 μM [RuCl₂(PPh₃)L²]; Lane 7: DNA + 60 μM H₂O₂ + 30 μM [RuCl₂(PPh₃)L³]; Lane 8: DNA + 60 μM H₂O₂ + 60 μM [RuCl₂(PPh₃)L³]; Lane 9: DNA + 60 μM H₂O₂ + 30 μM [RuCl₂(PPh₃)L⁴]; Lane 10: DNA + 60 μM H₂O₂ + 60 μM [RuCl₂(PPh₃)L⁴].

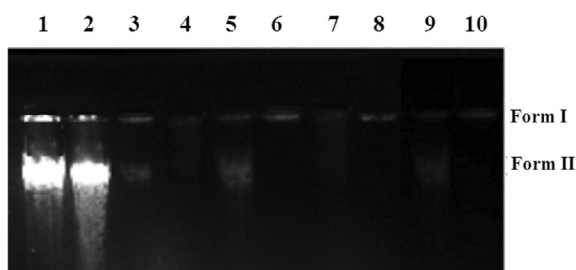


Figure 4 The gel electrophoresis showing the chemical nuclease activity of CT-DNA incubated at 37 °C for 4 h with different concentration of complexes in the presence of H₂O₂ as an oxidant; Lane 1: DNA alone; Lane 2: DNA + 60 μM H₂O₂; Lane 3: DNA + 60 μM H₂O₂ + 30 μM [RuCl₂(AsPh₃)L¹]; Lane 4: DNA + 60 μM H₂O₂ + 60 μM [RuCl₂(AsPh₃)L¹]; Lane 5: DNA + 60 μM H₂O₂ + 30 μM [RuCl₂(PPh₃)L²]; Lane 6: DNA + 60 μM H₂O₂ + 60 μM [RuCl₂(PPh₃)L²]; Lane 7: DNA + 60 μM H₂O₂ + 30 μM [RuCl₂(PPh₃)L³]; Lane 8: DNA + 60 μM H₂O₂ + 60 μM [RuCl₂(PPh₃)L³]; Lane 9: DNA + 60 μM H₂O₂ + 30 μM [RuCl₂(PPh₃)L⁴]; Lane 10: DNA + 60 μM H₂O₂ + 60 μM [RuCl₂(PPh₃)L⁴].

in the presence of varying concentrations of complexes for 48 h. The inhibitory concentration 50 (IC₅₀), is defined as the concentration required to reduce the size of the cell population by 50%. The IC₅₀ values are 178, 123, 149, 85 μM for complexes [RuCl₂(AsPh₃)L¹], [RuCl₂(PPh₃)L²], [RuCl₂(PPh₃)L³] and [RuCl₂(PPh₃)L⁴] respectively against the HeLa cell line. There are reports in the literature on the cytotoxic effects of the complexes with longer incubation time periods (72 h). The longer incubation period may result in the development of cellular resistance for that particular complex (Ramachandran et al., 2012). But, the data obtained for our complexes showed significant cytotoxicity with a short incubation period (48 h). Hence, our ruthenium(III) complexes show significant activity against the tumor cell line. However, these values are

lower than the standard anticancer drug cisplatin (IC₅₀ = 12.52 μM) (Krishnamorthy et al., 2011).

4. Conclusion

The benzothiazole substituted ferrocenyl thiosemicarbazone ruthenium(III) complexes were synthesized and characterized by various physico-chemical and spectroscopic methods. The complexes are tentatively assigned an octahedral geometry. The inhibition activity against some plant pathogenic fungal species and human pathogenic bacterial species of the thiosemicarbazone ligands exhibit good inhibition activity which is improved by the presence of the ruthenium moiety. The DNA binding study revealed that the complexes bind the DNA double helix *via* electrostatic interaction. Intrinsic binding constant of the complexes varies in the range of 1.0–3.6 × 10⁴ M⁻¹. From the intrinsic binding constant value, it is inferred that the complexes containing electron donating group bind strongly than the other complexes. On the other hand, the complex [RuCl₂(AsPh₃)L²] shows a dual mode of binding to DNA. DNA cleavage studies revealed that the complexes have the ability to cleave nucleic acids and the extent of the cleavage is found to be dose and incubation time dependent. These results should be valuable in understanding the mode of ruthenium(III) complexes with DNA as well as laying a foundation for the rational design of novel, powerful agents for probing and targeting nucleic acids. Moreover, the cytotoxicity evaluation *in vitro* shows that complexes displayed better antitumor activity against the selected cell line, HeLa with a short incubation period.

Acknowledgements

We sincerely thank the Council of Scientific and Industrial Research (CSIR), New Delhi, for financial support [Scheme. No. 01(2308)/09/EMR-II].

References

- Abd-Elzaher, M.M., Ali, I.A.I., 2006. *Appl. Organomet. Chem.* 20, 107.
- Alam, M., Khan, S., Khan, Md.S., 2008. *J. Chil. Chem. Soc.* 4, 1714.
- Arunachalam, S., Priya, N.P., Boopathi, K., Jayabalakrishnan, C., Chinnusamy, V., 2010. *Appl. Organomet. Chem.* 24, 491.
- Azza, A.A., Hussen, A., 2009. *Synth. React. Inorg. Met. Org. Chem.* 39, 13.
- Bechford, F.A., Leblanc, G., Thessing, J., Shaloski Jr., M., Frost, B.J., Li, L., Seeram, N.P., 2009. *Inorg. Chem. Commun.* 12, 1094.
- Biot, C., Taramelli, D., Forfar-Bares, I., Maciejewski, L.A., Boyce, M., Nowogrocki, G., Brocard, J.S., Basilico, N., Olliaro, P., Egan, T.J., 2005. *Mol. Pharm.* 2, 185.
- Chatt, J., Leigh, G.J., Mingos, D.M.P., Paske, R.J., 1968. *J. Chem. Soc. A*, 2636.
- Chitrapriya, N., Mahalingam, V., Zeller, M., Jayabalan, R., Swaminathan, K., Natarajan, K., 2008. *Polyhedron* 27, 939.
- Chitrapriya, N., Mahalingam, V., Zeller, M., Lee, H., Natarajan, K., 2010. *J. Mol. Struct.* 984, 30.
- Collinson, S.R., Fenton, D.E., 1996. *Coord. Chem. Rev.* 148, 19.
- Edwards, E.I., Epton, R., Marr, G., 1976. *J. Organomet. Chem.* 107, 351.
- Gimeno, M.C., Goitia, H., Laguna, A., Luque, M.E., Villacampa, M.D., 2011. *J. Inorg. Biochem.* 105, 1373.
- Hecht, S.M., 2000. *J. Nat. Prod.* 63, 158.

- Jaouen, G., Top, S., Vessieres, A., Leclercq, G., McGlinchey, M.J., 2004. *Curr. Med. Chem.* 11, 2505.
- Jeragh, B.J.A., Dissouky, A.E., 2005. *J. Coord. Chem.* 58, 1029.
- Krishnamorthy, P., Sathyadevi, P., Cowlwy, A.H., Butorac, R.R., Dharamaraj, N., 2011. *Eur. J. Med. Chem.* 46, 3376.
- Lawrence, D., Vaidyanathan, V.G., Unni Nair, B., 2006. *J. Inorg. Biochem.* 100, 1244.
- Leelavathy, L., Anbu, S., Kandaswamy, M., Karthikeyan, N., Mohan, N., 2009. *Polyhedron* 28, 903.
- Liu, X.W., Li, J., Deng, H., Zheng, K.C., Mao, Z.W., Ji, L.N., 2005. *Inorg. Chim. Acta* 358, 3311.
- Mahalingam, V., Chitrapriya, N., Fronczek, F.R., Natarajan, K., 2010. *Polyhedron* 29, 3363.
- Manimaran, A., Chinnusamy, V., Jayabalakrishnan, C., 2011. *Appl. Organomet. Chem.* 25, 87.
- Manivannan, S., Prabhakaran, R., Balasubramanian, K.P., Dhanabal, V., Karvembu, R., Chinnusamy, V., Natarajan, K., 2007. *Appl. Organomet. Chem.* 21, 952.
- Monks, A., Scudiero, D., Skehan, P., Shoemaker, R., Paull, K., Vistica, D., Hose, C., Langley, J., Cronise, P., Wolff, A.V., Goodrich, M.G., Campbell, H., Mayo, J., Boyd, M., 1991. *J. Natl. Canc. Inst.* 83, 757.
- Muthukumar, M., Sivakumar, S., Viswanathamurthi, P., Karvembu, R., Prabhakaran, R., Natarajan, K., 2010a. *J. Coord. Chem.* 63, 296.
- Muthukumar, M., Viswanathamurthi, P., Prabhakaran, R., Natarajan, K., 2010b. *J. Coord. Chem.* 63, 3833.
- Pandeya, S.N., Sriram, D., Nath, G., Declercq, E., 1999. *Eur. J. Pharm. Sci.* 9, 25.
- Perez, Z., Pauli, M., Bezerque, P., 1990. *Acta Biol. Med. Exp.* 15, 113.
- Prabhakaran, R., Anantharaman, S., Thilagavathi, M., Kaveri, M.V., Kalaivani, P., Karvembu, R., Dharmaraj, N., Bertagnolli, H., Dallermer, F., Natarajan, K., 2011. *Spectrochim. Acta Part A* 78, 844.
- Prasad, K.T., Therrien, B., Rao, K.M., 2010. *J. Organomet. Chem.* 695, 226.
- Pratviel, G., Pitie, M., Bernadou, J., Meunier, B., 1991. *Angew. Chem. Int. Ed. Eng.* 30, 702.
- Raja, N., Ramesh, R., 2010. *Spectrochim. Acta Part A* 75, 713.
- Raja, G., Sathya, N., Jayabalakrishnan, C., 2011. *J. Coord. Chem.* 64, 817.
- Ramachandran, E., Thomas, S.P., Poornima, P., Kalaivani, P., Prabhakaran, R., Padma, V.V., Natarajan, K., 2012. *Eur. J. Med. Chem.* 50, 405.
- Reddy, P.R., Shilpa, A., Raju, N., Raghavaiah, P., 2011. *J. Inorg. Biochem.* 105, 1603.
- Sampath, K., Jayabalakrishnan, K., 2013. *Synth. React. Inorg. Met. Org. Chem.* 43, 1279.
- Sharma, V.K., Srivastava, S., Srivastava, A., 2007. *Bioinorg. Chem. Appl.* 10 (article ID 68374).
- Singh, R.V., Joshi, S.C., Garaj, A., Naqpal, P., 2002. *Appl. Organomet. Chem.* 16, 713.
- Thangadurai, T.D., Natarajan, K., 2001. *Transition Met. Chem.* 26, 717.
- Trynda-Lemiesz, L., 2004. *Acta Biochim. Pol.* 51, 199.
- Venkatachalam, G., Ramesh, R., 2005. *Spectrochim. Acta Part A* 61, 2081.
- Venkatachalam, G., Raja, N., Pandiarajan, D., Ramesh, R., 2008. *Spectrochim. Acta Part A* 71, 884.
- Vogel, A.I., 1989. *Textbook of Practical Organic Chemistry*, fifth ed. Longman, London.
- Wang, Y., Yang, Z.Y., 2005. *Transition Met. Chem.* 30, 902.
- Wolfe, A., Shimer, G.H., Meehan, T., 1987. *Biochemistry* 26, 6392.